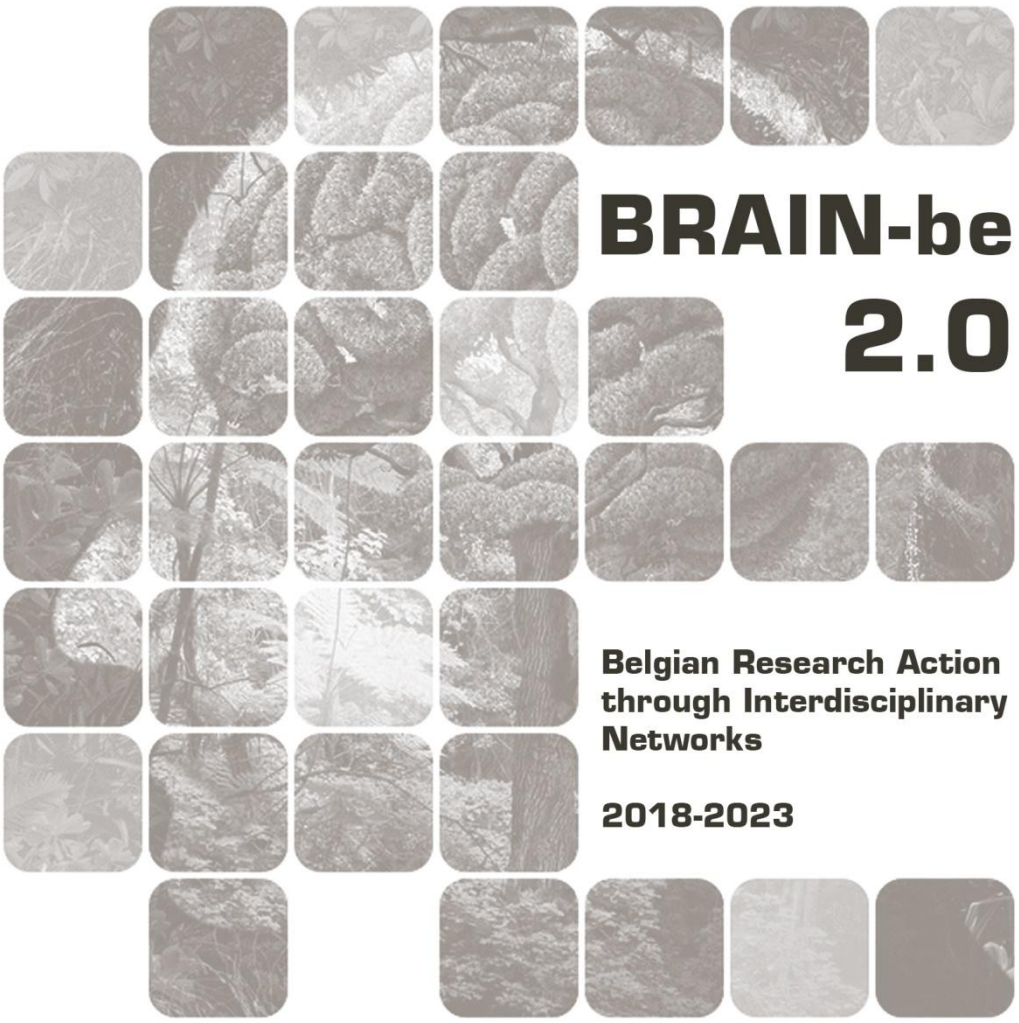

MUTER

Museum epigenomics as a Toolbox in Evolutionary Research

Vangestel Carl (Royal Belgian Institute of Natural Sciences) - Swaegers Janne (Royal Belgian Institute of Natural Sciences).

Pillar 2: Heritage science

belspo .be

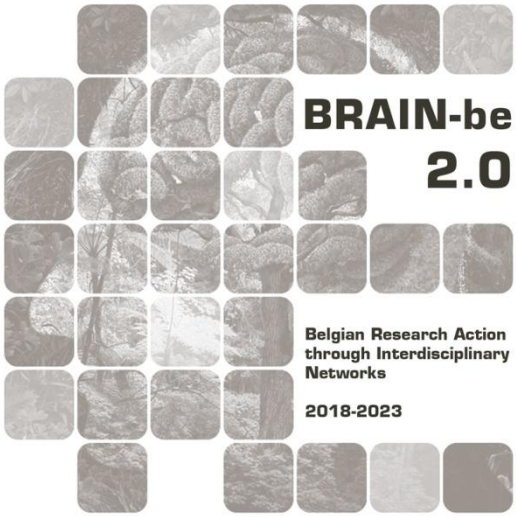

NETWORK PROJECT

MUTER

Museum epigenomics as a Toolbox in Evolutionary Research

Contract - B2/233/P2/MUTER

FINAL REPORT

PROMOTORS: Vangestel Carl (Royal Belgian Institute of Natural Sciences).

Jana Asselman (University of Ghent)

AUTHORS: Swaegers Janne (Royal Belgian Institute of Natural Sciences).

Vangestel Carl (Royal Belgian Institute of Natural Sciences).

natural sciences .be

belspo .be

Published in 2026 by the Belgian Science Policy Office
WTCIII
Simon Bolivarlaan 30 bus 7
Boulevard Simon Bolivar 30 bte 7
B-1000 Brussels
Belgium
Tel: +32 (0)2 238 34 11
http://www.belspo.be
http://www.belspo.be/brain-be

Contact person: Georges JAMART
Tel: +32 (0)2 238 36 90

Neither the Belgian Science Policy Office nor any person acting on behalf of the Belgian Science Policy Office is responsible for the use which might be made of the following information. The authors are responsible for the content.

No part of this publication may be reproduced, stored in a retrieval system, or transmitted in any form or by any means, electronic, mechanical, photocopying, recording, or otherwise, without indicating the reference:

Vangestel Carl, Janne Swaegers. Museum epigenomics as a Toolbox in Evolutionary Research. Final Report. Brussels: Belgian Science Policy Office 2023 – 29 p. (BRAIN-be 2.0 - (Belgian Research Action through Interdisciplinary Networks))

TABLE OF CONTENTS

ABSTRACT

Context

Epigenomics is among the fastest-growing and most dynamic fields in the life sciences. Despite the growing awareness of the unprecedented opportunities natural history collections have to offer and the increasing rate at which they are being mobilized for scientific purposes, to date natural history collections remain largely ignored for epigenomic research. While the Royal Belgian Institute of Naturals Sciences (RBINS) has a longstanding track record of conducting evolutionary research on both museum collections and contemporary samples, in-house epigenomic expertise to explore these resources is currently lacking at the RBINS.

Objectives

The primary objective of MUTER is to introduce technological and analytical epigenomic expertise at RBINS in order to strengthen and stimulate collection-based evolutionary research. Additionally, the project applies this expertise to investigate the role of DNA methylation in the adaptive evolution of *Calosoma* beetles and to evaluate the relative contributions of genetic determination and phenotypic plasticity to morphological adaptations in *Tectarius* snails.

Conclusions

Epigenomic wet-lab protocols and bioinformatic pipelines were successfully established for the analysis of museum specimens. We further demonstrated that samples preserved under suboptimal conditions can still yield high-quality data, confirming their value as a useful resource in museum epigenomic studies. While the *Calosoma* genome appears to lack DNA methylation, the investigation of open chromatin structures may offer a promising alternative approach. Adaptive shell morphology in snails showed no genetic basis, but instead appears to be driven by epigenetic mechanisms.

Keywords

Museum collections – Epigenomics – Evolution – Methylation – Genomics - Adaptation

1. INTRODUCTION

Epigenomics is one of the most rapidly evolving and booming fields in life sciences. It enhances our understanding of the **molecular mechanisms underpinning taxonomically and evolutionarily relevant phenotypic variation** by exploring how epigenetic signatures such as DNA methylation, histone modification or small RNAs may act as important drivers of phenotypic diversity. Interestingly, these modifications can be environmentally triggered and may mediate changes in gene expression levels within an individual, thereby allowing a single genotype to show remarkable phenotypic variation depending on its surrounding environment (phenotypic plasticity). These epigenetic processes may at least partly mirror the sometimes exceptional, and taxonomically confusing, intraspecific morphological variation observed in nature (Cavalli & Heard, 2019).

In general, genetic adaptation, i.e. the change in allele frequency through natural selection, is a rather slow evolutionary process that often can not keep up with the pace at which humans change the environment. This discrepancy may ultimately drive species to extinction when no other rescue mechanisms are at hand. One such mechanism often cited is the 'immediate' phenotypic plastic response to an environmental perturbation, which may even buy the necessary time for the organism to subsequently genetically adapt to this environmental change (Gibbin et al., 2017). Hence, in **a fast-**

evolving world epigenetic mechanisms may be of crucial importance in determining to what extent species are resilient to rapid habitat alterations and understanding to what extent genetic and epigenetic factors determine **the adaptive potential of species** may be **the crux of their long-term survival**. Moreover, evidence has accumulated that some epigenetic modifications may show transgenerational inheritance themselves, allowing populations to produce future generations that are instantaneously adapted to the altered environmental conditions (Bossdorf et al., 2008; Feil & Fraga, 2012; Jablonka, 2017). Even non-heritable epigenetic marks could facilitate adaptation by increasing the mutation rates at regions in the genome that are preferentially and recurrently targeted by epigenetic processes, ultimately leading to a phenotypic advantage and genetic variation that becomes selectable (Flores et al., 2013).

Notwithstanding the growing body of evidence on the role of epigenetics in developmental pathways and disease dynamics, **knowledge on the ecological and evolutionary impact of epigenetic processes is still in its infancy and many questions await to be answered**. In an ideal situation these processes should be mimicked and studied in lab settings, yet it is often difficult and unrealistic to fully grasp the complexity of all ecological and/or evolutionary interactions and lab conditions may induce physiological modifications to specimens. Within this framework, **natural history collections present exciting opportunities as they allow to explore and compare historic epigenomic patterns before and after an environmental change took place**. By granting us a window to the past, they provide unparalleled strong statistical designs to address these knowledge gaps (Hahn et al., 2020; Holmes et al., 2016; Kharouba et al., 2019; MacLean et al., 2018; Rubi et al., 2020). **These findings have stimulated the emergence of a new research field, 'museum epigenomics', which promises to redefine molecular research on biodiversity and to open a plethora of new research lines**(Hahn et al., 2020).

2. STATE OF THE ART AND OBJECTIVES

Despite the growing awareness of the unprecedented opportunities natural history collections have to offer and the increasing rate at which they are being mobilized for scientific purposes, to date **natural history collections are far from being exploited to the fullest** (Holmes et al., 2016; Kharouba et al., 2019; MacLean et al., 2018). Museum collections, such as those of RBINS, harbor a vast reservoir of information on the molecular mechanisms underlying biological diversity, but **unlocking these 'hidden treasures' remains a daunting task**. Only recently researchers have begun to utilise this genetic repository thanks to ground-breaking advancements in next-generation sequencing technology (Metzker, 2010). While museum studies on the spatial and/or temporal variability of nucleotide sequences have greatly advanced our understanding on the molecular basis of phenotypic variation, they have remained largely ignorant on exploring other important drivers of phenotypic diversity such as screening epigenetic modifications of DNA in historical samples (Bi et al., 2013; Hahn et al., 2020). Studying the epigenomes of such samples is however far from straightforward as DNA will typically endure a variety of post-mortem alterations like deamination, fragmentation, loss and exogenous contamination, which all complicate the implementation of standard epigenetic lab protocols (Rubi et al., 2020; Yeates et al., 2016). Notwithstanding a variety of epigenetic markers have been described and studied, **cytosine methylation seems the most promising candidate for epigenomics studies of museum collections** as this sort of epigenetic modification shows much less post-mortem decay(Llamas et al., 2012). Because cytosine methylation remains stable over extensive time periods, the main constraint in methylation protocols for historical DNA samples is to obtain DNA

of sufficient quality and quantity to allow amplification (Llamas et al., 2012). However, DNA extraction of historical samples and subsequent library construction for next-generation sequencing have been successfully applied in a range of taxa, and protocols continue to advance (Bi et al., 2013; Carøe et al., 2018; Rubi et al., 2020; Sproul & Maddison, 2017).

Methylation in eukaryotes can interfere in various ways with transcriptional processes (Feil & Fraga, 2012). Although the exact mechanism remains yet to be resolved, methylation can suppress transposon activity or affect chromatin condensation, thereby controlling gene expression through either inhibiting or enhancing access of the transcriptional machinery to DNA (Jimenez-Useche & Yuan, 2012; Schübeler, 2015). Numerous studies have nevertheless highlighted circumstantial evidence for the ecological or evolutionary role of DNA methylation by linking differentially methylated regions to phenotypic variation (Muyle et al., 2021; Skinner et al., 2014; Xu et al., 2020). By combining information on methylome, genome and morphology, this project aims to further contribute to the ultimate goal of exploring phenotypic and functional variation in museum collections. As an overarching goal of this project we intend to **bring in a new expertise, museum epigenomics, in line with RBINS Research Strategy which will provide researchers of RBINS the opportunity to complement existing morphological and genomic data with a new epigenomic data layer and to stimulate new research avenues** through internal and external JEMU (Joint Experimental Molecular Unit) collaborations. Within this framework we will apply this technology on two case studies, one on a unique adaptive radiation of *Calosoma* beetles at the Galápagos islands and another on a shell polymorphism of the intertidal periwinkle *Tectarius striatus* at the Azores and Cape Verde islands.

RBINS has a **longstanding track record of conducting evolutionary research on adaptive radiations with a specific focus on those occurring at the Galápagos** (De Busschere et al., 2012, 2015; Hendrickx et al., 2015; Van Belleghem et al., 2018)**.** A most intriguing radiation is those of the *Calosoma* beetles. Here, representatives of this genus radiated repeatedly into a highland and lowland ecotype along an altitudinal gradient replicated on all major islands. Although these islands strongly differ in age (0.5 MY – 3.5 MY) they share a pronounced difference in vegetation composition along altitudinal gradients, which has promoted adaptation and speciation in numerous invertebrate genera (De Busschere et al., 2012; Desender & de Dijn, 1990). This species complex has been sampled intensively between 1970 and 2014 during 17 field expeditions. The radiation has been studied extensively at RBINS and this project further builds on the former Belspo Pioneer project 'GENESORT' (refnr BR/121/PI/GENESORT, 'Is evolution repeatable? Introducing novel tools to unravel the genetics of parallel radiations'). Of the four *Calosoma* species endemic to the Galápagos, three are restricted to the high altitude vegetation zone of the islands San Cristobal (*C. linelli*), Santa Cruz (*C. leleuporum*) and Santiago (*C. galapageium*) and share several phenotypic similarities, such as a smaller overall size and in particular a strong reduction in size of traits related to dispersal (e.g. wing size reduction) (Desender & de Dijn, 1990). The fourth species, *C. granatense,* is a larger, long winged and highly dispersive species that occurs chiefly in lowland habitats of virtually all islands in the archipelago. Remarkably, on the largest and more recent islands Isabela and Fernandina, situated in the western part of the Galápagos, it is also abundant at higher elevations where it shows a reduction in wing size in line with the highland species (Figure 1). Extensive genomic data of this radiation is already available (including a reference genome, RADseq and whole-genome resequencing data, NCBI BioProject ID PRJNA706924) (Vangestel et al., 2024). There is a clear divergence gradient between highland and

lowland species/populations that neatly correlates with the age at which the islands emerged. While the oldest islands (age 1MY – 4MY) harbour highland species that are genetically well-differentiated from the lowland species, volcano tops of the youngest islands (0.035 MY – 0.07 MY) harbour populations of the lowland species that show already a clear reduction in wing-size in line with the species differentiation seen on the older islands, but still without a strong genetic differentiation (Vangestel et al., 2024). Previous work on adaptive radiations of several model systems indicated that DNA methylation was associated with key evolutionary genes or genomic regions under natural selection, suggesting methylation may play an important role in adaptive radiations, especially in the early stages of divergence (Artemov et al., 2017; Skinner et al., 2014; Vernaz et al., 2021; Xu et al., 2020). Therefore, the *Calosoma* radiation is extremely interesting due to the aforementioned divergence gradient. Genetic divergence between species on the oldest island is strongest, while younger islands harbour 'species', or rather populations, that show only minor genetic divergence. Yet, these latter populations already show signatures of the typical morphological differentiation between highland (short-winged) and lowland (long-winged) ecotypes.

As a first exploration we aim to assess whether methylation patterns in the *Calosoma* radiation at the Galápagos are congruent with those patterns observed in other model systems, i.e. we will specifically test whether known key genomic regions underlying adaptive phenotype variation in *Calosoma* are enriched for differentially methylated regions. Collections spanning the entire radiation will allow us to **explore whether methylation levels are linked to known genomic regions under selection** (Vangestel et al., 2024) and whether such methylation enrichment is most prominent present in the younger divergences of this adaptive radiation suggesting an important role for DNA methylation in adaptive evolution.

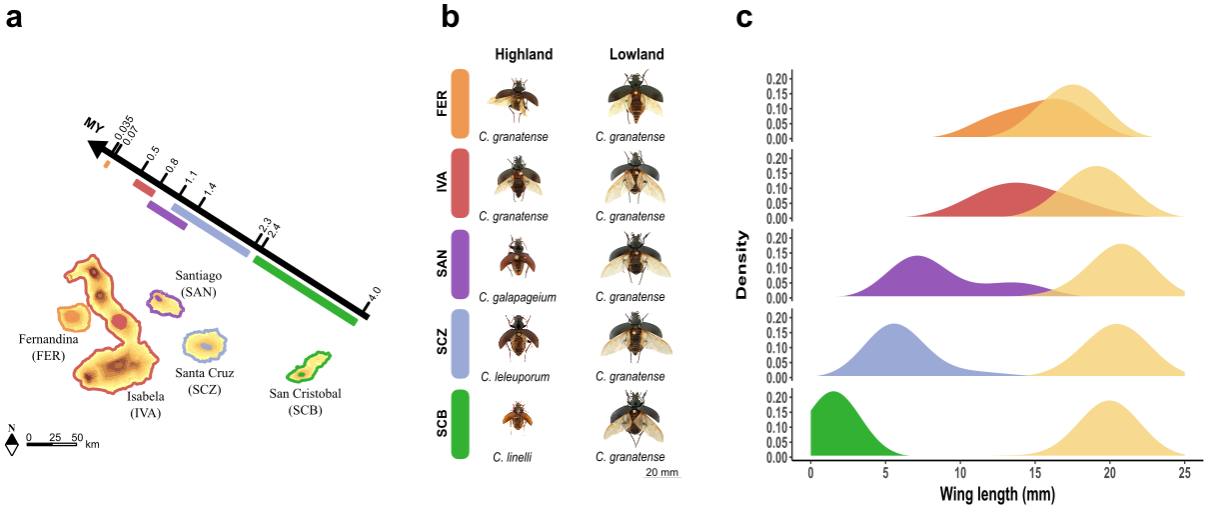

Figure 1. Caterpillar hunter beetles (*Calosoma*) *from the Galápagos. a) General view of the Galápagos islands and geographic location and age of the major islands, together with the distribution of the different species. b) General appearance of the different populations and species (left-side: highland ecotype, right-side: lowland ecotype). c) Wing size distribution, with lowland species depicted in yellow.*

Similarly, RBINS has a **longstanding track record of taxonomic and evolutionary research on molluscs, including the malacofauna of the Azores and Cape Verde** (De Wolf et al., 1997; Jordaens et al., 2009; Riel et al., 2005). As such, it harbours a vast, worldwide collection of molluscs. Many intertidal gastropods display remarkable intraspecific variation in shell morphology in response to environmental triggers (Clark et al., 2020). Indeed, shell size, shape, strength and sculpture of e.g. limpets, periwinkles and dog whelks are function of wave exposure, predation and heat/dessication

stress (Clark et al., 2020). Whether natural selection on genetic variants, phenotypic plasticity or an interaction between both provide the molecular foundation of this shell variation remains an open question (Clark et al., 2020). Natural selection is often, but not exclusively, considered as the main evolutionary force of shell variation in intertidal gastropods with a non-planktonic development and limited juvenile dispersal (Johannesson & Johannesson, 1996; Kess & Boulding, 2019; Le Pennec et al., 2017), whereas such genetic determinism seems less evident in species with a long-lived planktonic larval stage. Species within the latter group often show shell polymorphisms linked to environmental cues on a microgeographic scale, despite extensive gene flow between shell morphotypes (McMahon & Whitehead, 1987). These observations have fostered the idea that in such instances epigenetic variation may play an important role in local adaptation, but further research is much needed to substantiate this suggestion.

We will study a shell polymorphism of the planktonic developing periwinkle *Tectarius striatus* in the Azores and Cape Verde. Here two shell morphotypes of *Tectarius striatus* co-occur at a microgeographical scale, but display a non-random distribution across the landscape (De Wolf, Backeljau, Van Dongen, et al., 1998; De Wolf, Backeljau, & Verhagen, 1998; De Wolf et al., 1997; Van Den Broeck et al., 2008). The 'nodulose' morphotype has a highly sculptured and lighter shell with a smaller aperture, and predominates at wave-sheltered areas. In contrast, the 'smooth' morphotype bears heavier shells with few if any nodules and a larger aperture, and is most commonly observed at wave-exposed areas (Figure 2) (De Wolf, Backeljau, Van Dongen, et al., 1998; De Wolf et al., 1997). These habitat-related shell morphologies resemble different functional strategies. Wave dislodgment risk is minimized through an increased aperture, allowing to accommodate a larger foot muscle for optimal holdfast on substrates, and smoothening of the shell surface reduces drag forces. Smaller and more nodulose shells mitigate heat and dessication stress through a reduced contact area between shell and substrate (because of the smaller aperture of nodulose shells) and increased convection and reflection surface (De Wolf et al., 1997). Notwithstanding a clear spatial separation of both morphotypes, previous research indicated extensive gene flow between both 'nodulose' and 'smooth' *Tectarius striatus* populations (De Wolf, Backeljau, & Verhagen, 1998). Translocation experiments within such a shared gene pool showed that specimens rapidly increased aperture height when translocated from sheltered lagoons to wave-exposed areas, strongly suggesting that at least some morphological shell traits in *Tectarius striatus* have an epigenetic basis (De Wolf et al., 1997). While epigenetic studies on molluscs remain scant, some studies have been able to link variation in methylation levels to differences in salinity, temperature, chemical composition, infection rate or other habitat characteristics (Clark et al., 2018; Fallet et al., 2020; Thorson et al., 2017). Within this framework we will scan both the methylome and genome of 'smooth' and 'nodulose' populations to **associate both genetic and epigenetic variation to morphotype, so as to gain more insight into the molecular basis of shell morphology in this species**.

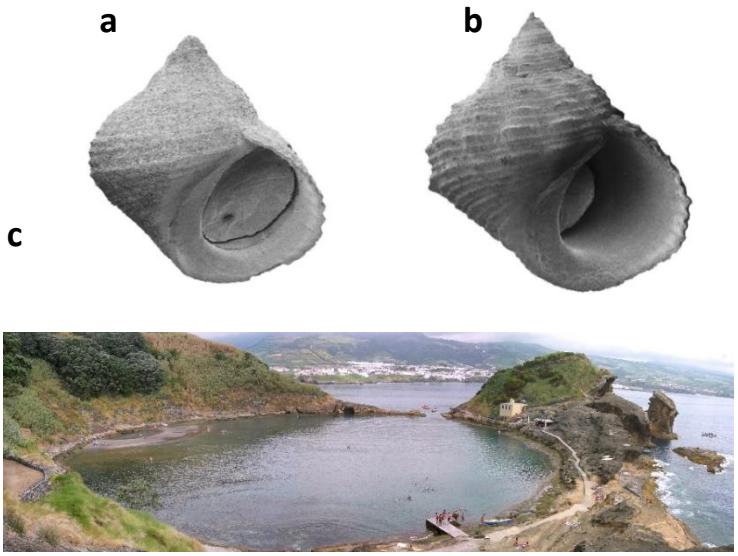

Figure 2. Tectarius striatus. Examples of a) 'smooth' morphotype and b) 'nodulose' morphotype, c) Example of a setting where the smooth and nodulose shell morphotypes of T. striatus show a different microgeographic distribution in the Azores (Ilheu de Vila Franca do Campo), with a sheltered lagoon and wave-exposed rocky shore at the outside.

In summary, in MUTER the aims are twofold. First, we will explore the feasibility of applying bisulphite NGS sequencing methods on museum repositories to assess their methylation profiles. In a second phase, we will implement this technology in two well-studied evolutionary research models.
Hence, more specifically the objectives of MUTER are:
i) to **bring** the technological and analytical **epigenomic expertise into the RBINS** to target the methylome of museum samples.
ii) to apply this expertise on two study systems to obtain a first exploration of:

- **the role of methylation in adaptive evolution** by exploring whether known genomic regions under genetic selection are enriched for differentially methylated regions using the *Calosoma* adaptive radiation.
- t**he role of genetic determinism and phenotypic plasticity in shell variation** in *Tectarius striatus* in response to differential wave exposure by linking genetic, epigenetic and morphological variation.

iii) to **stimulate new collection-based research** lines in various scientific fields through future internal and external JEMU collaborations.

3. METHODOLOGY

3.1. Library preparation

While several methods are available to assess the level of cytosine methylation in the genome, whole genome bisulfite-sequencing (WGBS) has become the golden standard to detect such DNA methylation patterns. During the bisulfite reaction of DNA, unmethylated cytosine is converted to uracil, while methylated cytosines remain unaffected by the bisulphite treatment (Grehl et al., 2018). After PCR amplification uracils (i.e. originally unmethylated cytosines) are translated to thymines. As a first step we screened the scientific literature on the latest and most advanced commercial bisulfite conversion kits. We selected a combination of the EZ DNA Methylation-Gold Kit (Zymo, #D5005) and the xGen™ Methyl-Seq Lib Prep (IDT, # 10009824) for respectively bisulfite conversion and NGS library preparation. The latter kit is also easily adjustable to allow implementing a reduced-representation approach where genomes are first digested by a restrictions enzyme (MspI, New England Biolabs) (RRBS) and DNA is sequenced in small adjacent regions up- and downstream of the restriction site. Such approaches could be useful when aiming to sequence the DNA of a large number of samples by reducing the sequencing costs.

DNA was extracted using the Nucleospin Tissue Kit (Macherey-Nagel GmBH) following the manufacturer's protocol, after which a total amount of 332 ng DNA per sample was sheared to an average fragment size of ~350 bp using the Covaris M220 Focused-ultrasonicator at the Nucleomics Core (VIB, Belgium) (80s duration, 50W peak incident power, 20% duty factor, 200 cycles per burst). Thereafter 133ng of fragmented DNA was used as an input for the bisulfite treatment and NGS library preparation. In brief, the latter entails an adaptase, extension and PCR step. The adaptase step simultaneously performs end repair, tailing, and ligation of an adapter to the 3' end of each single-stranded DNA fragment. The subsequent extension step ligates an adapter at the 5' end while the PCR step provides a unique index to each library during amplification.

3.2. Bisulfite conversion rate

To calculate the bisulfite conversion rate, unmethylated reference DNA (lambda phage DNA, Promega, #D1521) was added to samples prior to DNA shearing, at a ratio of 0.1% (w/w) of the total DNA. Lambda phage DNA is completely unmethylated therefore every cytosine position is expected to be converted to a uracil during bisulfite treatment. The ratio of the number of uracil-converted cytosines over total cytosines is assigned as the bisulfite conversion success rate. After sequencing reads were mapped to the lambda phage reference genome (GenBank accession no. J02459) using Bismark (Krueger & Andrews, 2011), mapped reads extracted and submitted to the bioinformatical pipeline to assess the methylation state of cytosines (see below).

3.3. Optimalisation library preparation

We ran a small pilot experiment to assess the most optimal number of PCR cycli (6,9, 10 or 30 cycli) to amplify our NGS libraries. The most optimal number of PCR cycli was chosen in such a way it minimized the number of cycli (which induces PCR replicates) while still yielding sufficient DNA after amplification (>5ng/µl, expected fragment size of 500bp).

3.4. Sampling

3.4.1 *Calosoma* specimens

During the reproductive phase, especially female long-winged *Calosoma* beetles may undergo histolysis of energetically demanding flight muscles and reallocate the released resources into fat

storage. As methylation profiles are tissue specific we dissected the thorax of *Calosoma* specimens and assigned the specimens according to the muscle - fat ratio into three three classes: predominantly fat tissue, predominantly muscle tissue or a mixture of fat and muscle tissue (Figure 3).

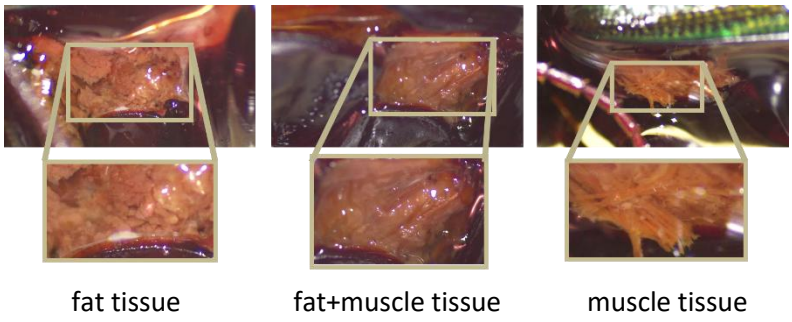

Figure 3. Illustration of the different proportions of fat versus flight muscles found in thoraces of Calosoma specimens.

WGBS libraries were prepared for 10 *Calosoma* specimens that were stored at -80°C (Table I). For three samples we prepared libraries of each side of the thorax to ascertain no differences between thorax sides were present, as preferentially only one side of the thorax would be used, allowing the other part of the body to be used for complementary analyses (for example RNA Seq) in the future. We also added three technical replicates (libraries of identical samples, left side of the thorax) to assess the repeatability of methylation calling.

TABLE I. Sample info and WGBS library conditions of *Calosoma* specimens

Sample identifier		Shearing		Bisulphite conversion	Library preparation			
Sample ID	DNAID	Concentration (ng/µl)	Quantity (ng)	Quantity (ng)	Concentration (ng/µl)		#PCR cycli	Index
					Pre PCR	Post PCR		
K1.2.37.L	1L.1	60.8	332.5	133	0.55	10.4	9	idt_udi_A1
K1.2.37.L	1L.2	60.8	332.5	133	0.59	20	9	idt_udi_B1
K1.2.37.R	1R	54.4	332.5	133	0.4	14.8	9	idt_udi_C1
K1.2.38.L	2L.1	27.4	332.5	133	1.08	16.7	9	idt_udi_E1
K1.2.38.L	2L.2	27.4	332.5	133	0.95	19.5	9	idt_udi_F1
K1.2.38.R	2R	33.6	332.5	133	0.71	18.2	9	idt_udi_G1
K1.2.39.L	3L.1	21.8	332.5	133	0.84	16.2	9	idt_udi_H1
K1.2.39.L	3L.2	21.8	332.5	133	0.73	20.8	9	idt_udi_C2
K1.2.39.R	3.R	18.8	332.5	133	0.46	13.1	9	idt_udi_D2
K1.1.44	4	63.6	332.5	133	0.39	13.8	9	idt_udi_E2
K1.1.45	5	7.28	332.5	133	0.71	13.4	9	idt_udi_G2
K1.3.64	6	31.4	332.5	133	0.43	10.2	9	idt_udi_H2
K1.3.65	7	27.6	332.5	133	0.33	12.2	9	idt_udi_A3
K1.3.66	8	56.4	332.5	133	0.5	14.1	9	idt_udi_B3
K1.3.7	9	33.4	332.5	133	0.31	9.94	9	idt_udi_C3
K1.3.8	10	50.8	332.5	133	0.16	5.82	9	idt_udi_D3

Overview of sequenced libraries of *Calosoma* specimens. Table depicts the concentration and/or quantity of DNA during shearing, bisulphite conversion and PCR amplification. The extensions '.L' and '.R' in SampleID refer to respectively left and right side of the thorax.

3.4.2 *Tectarius striatus* specimens

WGBS libraries were constructed from the homogenous foot tissue of 30 *Tectarius striatus* specimens (stored at -80°C). Samples were collected at the Azores (n=8) and Cape Verde (n=22) and each morphotype (nodulose vs. smooth) was represented equally (n=15) in the dataset (Table II). For comparative purposes we also constructed a RRBS library of two specimens and assessed to what extent mean methylation levels were similar in both sequencing approaches.

Prior to DNA extraction, radula and reproductive organs were removed to minimize the inclusion of exogenous DNA. Eight samples (4 of each morphotype, equally spread over the Azores and Cape Verde islands) were selected for whole-genome resequencing to characterize nucleotide variation across locations and morphotype. We further selected less optimal museum specimens that were stored at room temperature in ethanol for three decades (Table III) to assess if inferior storage conditions in museum collections affect methylation signatures.

Table II. Sample info and WGBS library conditions of *Tectarius striatus* specimens

Sample identifier		Location	Morphotype	Shearing		Bisulphite conversion	Library preparation			
Sample ID	DNAID			Concentration (ng/µl)	Quantity (ng)	Quantity (ng)	Concentration (ng/µl) Pre PCR	Concentration (ng/µl) Post PCR	#PCR cycli	Index
S.3	S.3	Cabo Verde, Mindelo (Wall II)	smooth	21.2	332.5	133	too low	3.16	9	idt_udi_D1
S.4	S.4	Cabo Verde, Mindelo (Wall II)	smooth	41.8	332.5	133	NA	12.5	9	idt_udi_F2
S.5	S.5	Cabo Verde, Mindelo (Wall II)	smooth	27.8	332.5	133	NA	9.26	9	idt_udi_G4
S.7	S.7	Cabo Verde, Mindelo (Wall II)	nodulose	47	332.5	133	NA	9.32	9	idt_udi_H4
S.8^{R}	S.8	Cabo Verde, Mindelo (Wall II)	nodulose	69.8	332.5	133	NA	11.6	9	idt_udi_A5
S.9	S.9	Cabo Verde, Mindelo (Wall II)	nodulose	32.6	332.5	133	NA	8.88	9	idt_udi_B5
S.10^{R}	S.10	Cabo Verde, Mindelo (Wall II)	nodulose	61.2	332.5	133	NA	12	9	idt_udi_C5
S.23	S.23	Cabo Verde, Mindelo (Morro Branco)	smooth	47.6	332.5	133	0.17	10.7	9	idt_udi_D5
S.24	S.24	Cabo Verde, Mindelo (Morro Branco)	smooth	45.8	332.5	133	0.12	8.18	9	idt_udi_E5
S.25	S.25	Cabo Verde, Mindelo (Morro Branco)	smooth	19.7	332.5	133	0.43	12.9	9	idt_udi_F5
S.26	S.26	Cabo Verde, Mindelo (Morro Branco)	smooth	38.8	332.5	133	0.11	9.98	9	idt_udi_G5
S.27	S.27	Cabo Verde, Mindelo (Morro Branco)	nodulose	27	332.5	133	0.29	7.26	9	idt_udi_H5
S.29	S.29	Cabo Verde, Mindelo (Morro Branco)	nodulose	15.6	332.5	133	0.43	6.82	9	idt_udi_A6
S.30	S.30	Cabo Verde, Mindelo (Morro Branco)	nodulose	15.05	332.5	133	0.43	11.1	9	idt_udi_B6
S.31^{W}	S.31	Cabo Verde, Mindelo (Shipwreck I)	smooth	44.4	332.5	133	0.37	9.94	9	idt_udi_C6
S.32^{W}	S.32	Cabo Verde, Mindelo (Shipwreck I)	smooth	41.6	332.5	133	0.39	11.4	9	idt_udi_D6
S.33	S.33	Cabo Verde, Mindelo (Shipwreck I)	smooth	55.8	332.5	133	0.48	13.4	9	idt_udi_E6
S.34	S.34	Cabo Verde, Mindelo (Shipwreck I)	smooth	25.4	332.5	133	0.90	7.96	9	idt_udi_F6
S.35	S.35	Cabo Verde, Mindelo (Shipwreck I)	nodulose	46.6	332.5	133	0.55	10.5	9	idt_udi_G6
S.36^{W}	S.36	Cabo Verde, Mindelo (Shipwreck I)	nodulose	45.6	332.5	133	0.49	12.6	9	idt_udi_H6
S.37^{W}	S.37	Cabo Verde, Mindelo (Shipwreck I)	nodulose	48.2	332.5	133	0.40	12.8	9	idt_udi_A7
S.38	S.38	Cabo Verde, Mindelo (Shipwreck I)	nodulose	23.2	332.5	133	0.17	2.72	9	idt_udi_C8
S.39	S.39	Azores, Faial, Capelhinos	smooth	11.35	332.5	133	too low	2.92	9	idt_udi_C7
S.40^{W}	S.40	Azores, Faial, Capelhinos	smooth	25.4	332.5	133	0.44	6.74	9	idt_udi_D7
S.41^{W}	S.41	Azores, Faial, Capelhinos	smooth	22.2	332.5	133	0.11	7.92	9	idt_udi_E7
S.42	S.42	Azores, Faial, Capelhinos	smooth	21.8	332.5	133	0.38	3.96	9	idt_udi_F7
S.43	S.43	Azores, Faial, Capelhinos	nodulose	56.4	332.5	133	0.30	3.98	9	idt_udi_G7
S.44^{W}	S.44	Azores, Faial, Capelhinos	nodulose	44	332.5	133	0.41	6.2	9	idt_udi_H7
S.45^{W}	S.45	Azores, Faial, Capelhinos	nodulose	51.8	332.5	133	0.27	5.18	9	idt_udi_A8
S.46	S.46	Azores, Faial, Capelhinos	nodulose	33	332.5	133	0.38	4.3	9	idt_udi_B8

Overview of sequenced libraries of *Tectarius striatus* specimens. Table depicts the concentration and/or quantity of DNA during shearing, bisulphite conversion and PCR amplification. Genomes of samples indicated by 'W' have been resequenced (WGS), samples indicated by 'R' were included in the RRBS protocol.

Table III. Sample info and WGBS library conditions of seven less well preserved *Tectarius striatus* specimens

Sample identifier		Shearing		Bisulphite conversion	Library preparation			
Sample ID	DNAID	Concentration (ng/µl)	Quantity (ng)	Quantity (ng)	Concentration (ng/µl) Pre PCR	Concentration (ng/µl) Post PCR	#PCR cycli	Index
S.E.1	S.E.1	118	332.5	133	0.27	3.5	9	idt_udi_G8
S.E.2	S.E.2	39.2	332.5	133	too low	2.16	9	idt_udi_H8
S.E.3	S.E.3	50.6	332.5	133	0.31	2.24	9	idt_udi_A9
S.E.4	S.E.4	106	332.5	133	0.232	3.5	9	idt_udi_B9
S.E.5	S.E.5	6.7	332.5	133	too low	1.97	9	idt_udi_C9
S.E.7	S.E.7	84	332.5	133	0.526	6.24	9	idt_udi_D9
S.E.8	S.E.8	53.6	332.5	133	0.29	4.64	9	idt_udi_E9

Overview of sequenced libraries of 7 *Tectarius striatus* specimens stored at room temperature in ethanol. Table depicts the concentration and/or quantity of DNA during shearing, bisulphite conversion and PCR amplification.

All libraries were quality-checked and quantified using Agilent 2100 Bioanalyzer. Sequencing was performed at Novogene (Germany) on an Illumina NovaSeq X Plus Series platform, generating 150 bp paired-end reads.

3.5. Bioinformatical pipeline and statistical analysis

Briefly, a quality control was performed on all sequencing reads using the FastQC and MultiQC software packages. Raw sequencing reads were trimmed to remove adapter contamination and low-quality bases according to the IDT xGen™ Methyl-Seq protocol. The resulting trimmed reads were aligned to the reference genome using abismal 3.2.2, a bisulphite-aware aligner optimized for WGBS data. Following alignment, PCR duplicates were identified and removed using the markdup function in samtools 1.15.1, ensuring that only unique reads were retained for downstream analyses. Cytosine methylation levels at single-base resolution were determined using MethylDackel 0.6.1, which extracts methylation information directly from bisulphite sequencing alignments. To assess genome-wide methylation patterns and identify differences between the smooth and nodulous morphotypes, we used the R package methylKit 1.26.0. Analyses included normalization of coverage across samples, filtering of low-coverage loci, and statistical testing for differentially methylated sites between morphotypes using t-tests at a FDR<0.05. As no reference genome was available for *Tectarius striatus* we assembled a reference genome based on short-read sequence data. Paired-end Illumina WGS reads of sample S31 were first quality-trimmed using Trim Galore 0.6.10 to remove adapters and low-quality bases. Trimmed reads were then error-corrected using Lighter 1.1.3 (k-mer size = 17, genome size = 1.35 Gb) to reduce sequencing errors. The corrected reads were assembled de novo with MaSuRCA 4.1.4. The configuration used automated k-mer selection, paired-end scaffolding, and default CABOG overlap parameters. JF_SIZE was set to 3,000,000,000 to accommodate k-mer counting for a genome of approximately 1.5 Gb, ensuring sufficient hash space for Jellyfish during assembly.

Note: high-molecular weight DNA samples have been send to a sequencing facility for long-read sequencing (regular PacBio HiFi and Ampli-Fi protocol) that would improve the length and continuity of the reference genome assembly. So far this has been unsuccessful due to the sequencing inhibitors present in the mucus of snails (common problem in marine snails).

SNP calling in whole-genome resequenced specimens were done using BCFtools. The generated vcf file was subsequently filtered for biallelic SNPs, a MAF of 0.1, QUAL>30, allele depth between 30-50 and only SNPs with no missing data were retained (missing rate of 0%). Pairwise genetic differentiation between morphotypes (F_{ST}) were calculated using VCFtools. To minimize linkage disequilibrium among SNPs, we thinned the VCF such that only one SNP was retained within each 1000 bp window using VCFtools. Population structure was assessed using a PCoA using the R package adegenet. In addition, we aimed to delineate clusters (K) of individuals based on their multilocus genotypes using the software package Structure. We applied an admixture model with K = 1–4, 200 000 Markov Chain Monte Carlo repetitions, a burn-in period of 100 000, correlated allele frequencies and no prior information on the population of origin. To further evaluate the extent to which genotypes differentiate between morphotypes (smooth vs. nodulose) or populations (Azores vs. Cabo Verde), we performed a discriminant analysis of principal components (DAPC) using the R package adegenet.

4. SCIENTIFIC RESULTS AND RECOMMENDATIONS

4.1 Bisulphite conversion success

The bisulphite treatment during our library preparation appeared highly successful as more than 99.5% of all unmethylated cytosines of the Lambda DNA were successfully converted by the bisulphite treatment to uracils and thymines after PCR amplification. We therefore may assume with high confidence that very few methylated cytosines in our focal specimens will remain undetected after bisulphite treatment (Table IV).

TABLE IV. High conversion efficiency of unmethylated phage lambda DNA

Type	Average	SD
Conversion rate in CpG context	99.62%	0.05%
Conversion rate in CHG context	99.61%	0.05%
Conversion rate in CHH context	99.57%	0.06%

Average bisulphite conversion rate of all analysed C's in reads that aligned to the *Escherichia coli* phage lambda genome. All the samples contained an unmethylated lambda spike-in.

4.2 Optimal number of PCR cycli

Six PCR cycli did not obtain sufficient DNA (> 5ng/µl), while nine PCR cycli did reach the lower threshold. Hence, all subsequent libraries were prepared using nine PCR cycli.

TABLE V. Optimalisation number of PCR cycli

Sample identifier		Shearing		Bisulphite conversion	Library preparation			
Sample ID	DNAID	Concentration (ng/µl)	Quantity (ng)	Quantity (ng)	Concentration (ng/µl)		#PCR cycli	Index
					Pre PCR	Post PCR		
K1.3.64	6	31.4	332.5	133	0.42	1	6	idt_udi_F2
K1.2.37.R	1.R	54.4	332.5	133	0.43	1.58	6	idt_udi_G1
K1.2.37.A	1A	34.8	332.5	133	0.65	8.24	9	idt_udi_G2
K1.2.38.A	2A	36.6	332.5	133	0.44	9.78	10	idt_udi_D2
K1.2.37.A	1A	34.8	332.5	133	0.27	42.4	30	idt_udi_D1

Overview of non-sequenced libraries of *Calosoma* specimens used for optimalisation of the WGBS protocols. Table depicts the concentration and/or quantity of DNA during shearing, bisulphite conversion and PCR amplification.

4.3 Epigenomic variation underling a wing polymorphism in *Calosoma* beetles

After processing sequencing reads of all *Calosoma* specimens no methylation signature could be detected in any of the samples, i.e. no bases containing 100% methylation (Figure 4). This may indicate that either the genome of beetles is not methylated at all and therefore does not play a crucial role in differential wing development or that key genes are not methylated in adults (this study), but rather in other developmental (i.e. larval) stages. Unfortunately we did not have access to any larvae in our collections. Although the wetlab protocol and bioinformatical pipeline were successfully installed, due to the low methylation rates in *Calosoma* we decided not to further explore the use of this epigenetic marker in our case study on the role of epigenetics in an adaptive radiation of *Calosoma* beetles. Therefore, as a potential alternative and complementary epigenetic approach, we conducted a preliminary evaluation of ATAC-seq (Assay for Transposase-Accessible Chromatin sequencing) for its application in future epigenomic studies in collaboration with Prof. Dr. Van Belleghem's lab (KU Leuven). Briefly, ATACseq is a method to profile chromatin accessibility genome-wide. Using a Tn5 transposase it identifies open chromatin regions, parts of the genome where DNA is accessible because nucleosomes are absent or loosely packed. These regions could correspond to promotor, enhancer or transcription factor binding sites and therefore be actively involved in gene regulation.

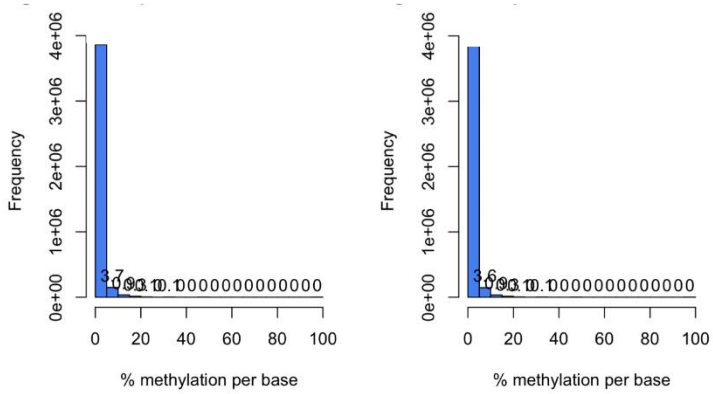

Figure 4. Percentage of methylation per base of forward reads (left panel) en reverse reads (right panel) of sample '1L'.

We prepared a library from a carabid beetle sample (*Pterostichus Niger*, a species of which ample supply is available in the collection) using a modified version of the original protocol of Buenrostro et al.(Buenrostro et al., 2015). A fragment analysis of the prepared library gave a pattern in concordance with the expected profile (Figure 5). Nucleosome-free regions (the most abundant ones) were typically centred around 100bp, while mononucleosome peaks located at 180-200 bp (the second distinct peak in Figure 5). Finally, a dinucleosome peak was detected at 360-400bp but, as often reported, at lower intensity. We are currently planning to apply the ATAC-seq protocol to *Calosoma* test samples and will further optimize the procedure by including the use of a flow cytometry for cell counting to enhance standardization.

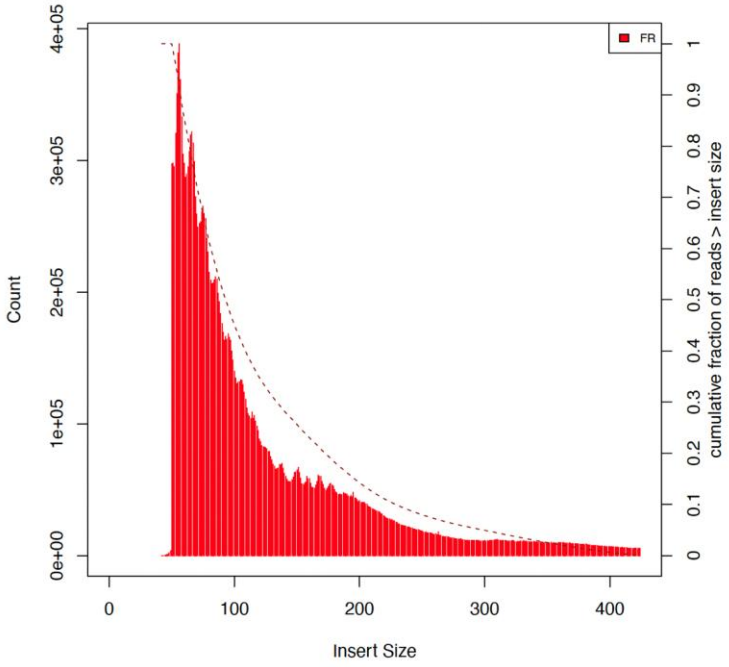

Figure 5. Histogram of insert sizes of the ATAC-seq sequencing data. The first peak (50bp) corresponds to where the Tn5 transposase inserted into nucleosome-free regions. The second small peak (towards 200bp) corresponds to where Tn5 inserted around a single nucleosome. The bump towards 400bp is where Tn5 inserted around two adjacent nucleosomes. FR=forward reverse read orientation.

4.4 Genetic and epigenetic variation underlying morphotype differentiation in *Tectarius striatus*

4.4.1 Genomics of *Tectarius striatus*

The masurca assembled draft genome had a total length of 875,619,763bp. It consisted of 946091 scaffolds and had an N50 value of 1116bp. While this draft genome was still highly fragmented, as we could only rely on short read sequencing data (see note 3.4), 86%-95% of the sequenced reads of each sample still mapped to this reference genome. An overview of the read alignment metrics for each sample is given in Table VI.

TABLE VI. Read alignment metrics for each of the resequenced samples.

Metric	S31	S32	S36	S37	S40	S41	S44	S45
Total reads	256,537,315	251,366,490	220,072,393	244,763,801	266,087,655	210,897,917	209,872,790	231,774,735
Mapped reads	243,691,725 (94.99%)	224,709,669 (89.40%)	190,895,508 (86.74%)	215,747,503 (88.15%)	234,676,013 (88.20%)	180,871,403 (85.76%)	181,318,564 (86.39%)	201,601,537 (86.98%)
Paired in sequencing	256,537,315	251,366,490	220,072,393	244,763,801	266,087,655	210,897,917	209,872,790	231,774,735
Read1	128,092,481	125,662,566	110,032,247	122,379,350	133,031,519	105,455,959	104,972,119	115,910,089
Read2	128,444,834	125,703,924	110,040,146	122,384,451	133,056,136	105,441,958	104,900,671	115,864,646
Properly paired	185,536,042 (72.32%)	152,511,466 (60.67%)	132,569,794 (60.24%)	150,907,078 (61.65%)	160,127,006 (60.18%)	127,646,454 (60.53%)	129,417,753 (61.66%)	139,957,464 (60.39%)
With itself & mate mapped	238,029,191	211,908,102	178,600,458	202,818,891	220,142,660	168,735,425	169,477,804	188,087,221
Singletons	5,662,534 (2.21%)	12,801,567 (5.09%)	12,295,050 (5.59%)	12,928,612 (5.28%)	14,533,353 (5.46%)	12,135,978 (5.75%)	11,840,760 (5.64%)	13,514,316 (5.83%)
Mate mapped to different chr	49,262,429	56,847,410	43,938,123	49,601,922	57,390,437	39,152,686	38,172,420	45,966,192
Mate mapped to different chr (mapQ≥5)	26,667,810	23,096,676	19,061,019	21,279,267	24,001,013	17,693,171	17,671,436	20,898,631

One specimen (smooth morphotype, Capo Verde) resulted in aberrant patterns in downstream analyses and genetic metrics, and was therefore discarded as a conservative measure.

The first principal component (PCoA1) explained 18.6% of the total variation, while the second principal component (PCoA2) explained 17.0%. Samples were separated by population along the first PCoA axis (PCoA1). The second axis distinguished variation among samples within the Azores. Notably, no clear separation among morphotypes was detected based on genetic variation (Figure 6).

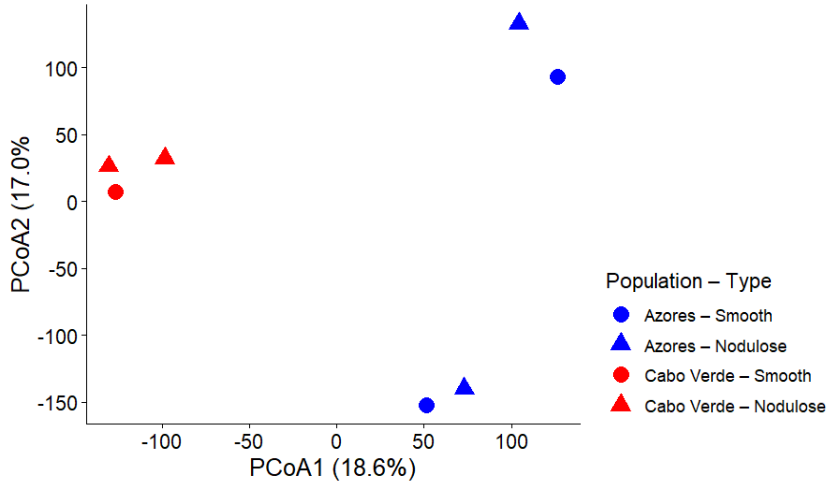

Figure 6. PCoA of genetic variation of nodulose (triangle) and smooth (circle) specimens of the Azores (blue) and Cabo Verde (red). The percentage of variation explained by each axis is given between brackets.

A Structure analysis further corroborated the PCoA analysis as it identified the Azores and Cabo Verde as two distinct genetic clusters (K=2) (Figure 7, upper panel). Considering more subclusters separated again the Cabo Verde populations, but not according to morphotype (K=3, K=4) (Figure 7, middle and lower panel).

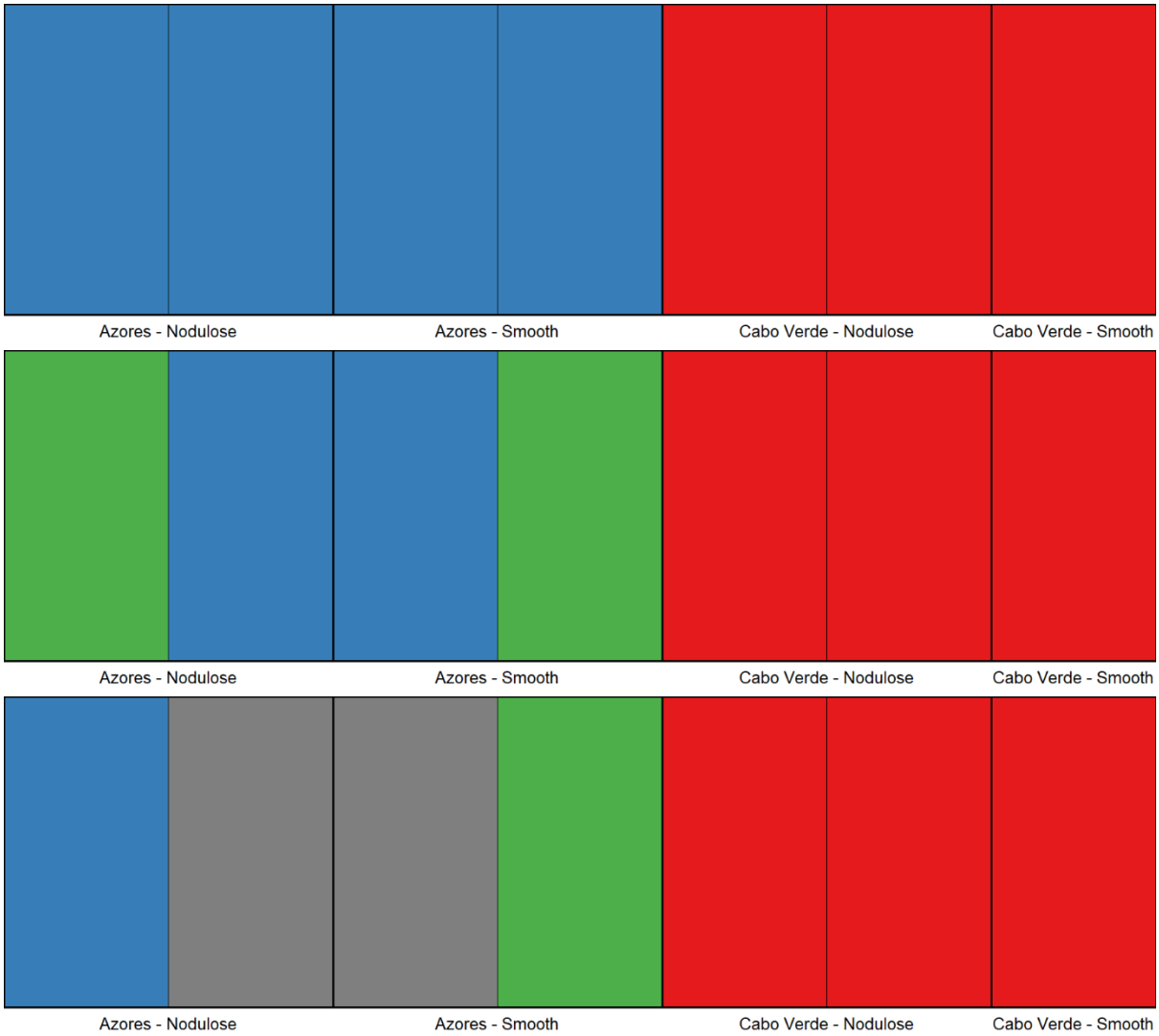

Figure 7. Structure plot for both shell morphotypes in the different T. striatus populations of the Azores and Cabo Verde islands. Each bar represents an individual partitioned according to his admixture proportions from genetic clusters. Upper panel: k=2, middle panel: K=3, and lower panel: K=4.

The DAPC analysis indicated strong genetic differentiation among both populations (Azores vs. Cabo Verde) as the first discriminant function fully separated both populations (Figure 8, left panel). In contrast, the analysis suggested limited discriminative power between morphotypes as illustrated by the extensive overlap between both morphotypes in the density plot (Figure 8, right panel). While only a limited number of samples per group were available and hence the results need to be interpreted cautiously, they did corroborate previous findings.

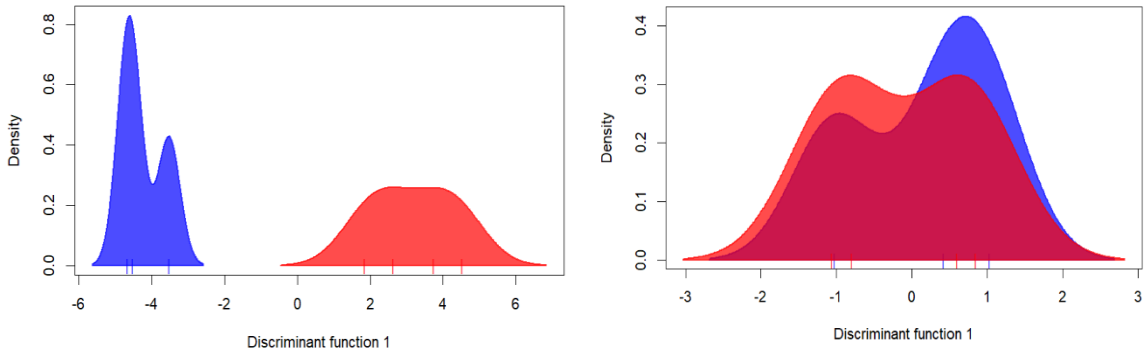

Figure 8. Density plot of the first discriminant axis of the DAPC analysis based on genomic variation depicting differentiation among islands (left figure) and morphotypes (right figure).

In line with previous results, we observed on average little genetic differentiation between morphotypes as indicated by the low Weir and Cockerham weighted Fst estimate (F_{ST} = -0.0054). We also observed very few outlying genomic windows ($F_{ST,window}$ > mean F_{ST} + 3 x standard deviation) indicating we had no strong evidence that variation at certain genomic regions may drive the observed phenotypic differences.

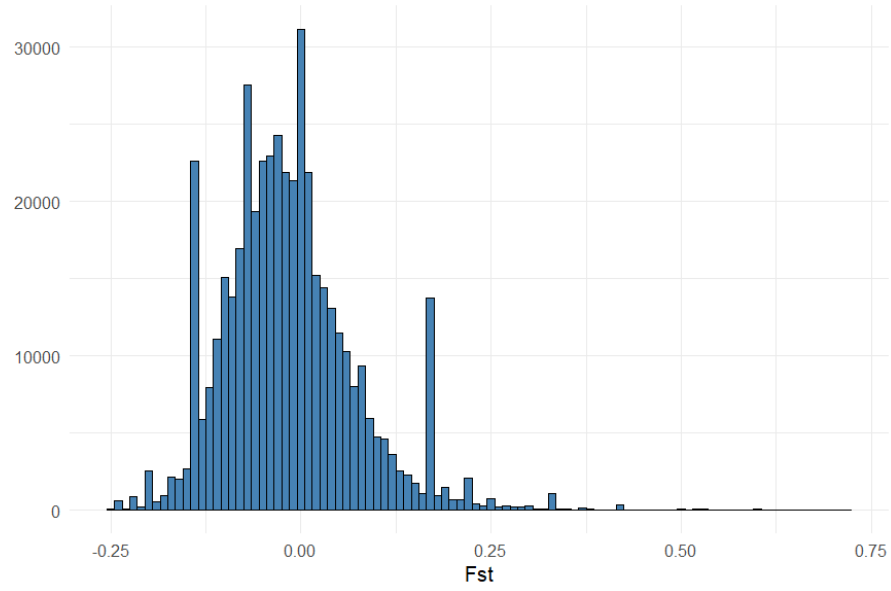

Figure 9. Histogram of F_{ST} values of 1000bp windows depicting genetic differentiating between morphotypes.

In summary, to date we have no strong indication that the observed shell variation in response to differential wave-exposure is genetically determined. Further analyses should however also include putative effects of structural genetic variation on shell morphotype.

4.4.2 Epigenomics of *Tectarius striatus*

We first sequenced and analysed the WGBS data of 7 pilot snails (comprising both smooth and nodulous morphotypes, S.3-S.10, see Table II). In contrast to the lack of methylation signatures in *Calosoma* beetles, a frequency plot of the percentage of methylation per base in *Tectarius striatus* showed the expected bimodal plot, indicating evidence of bases with complete methylation (Figure

10). After filtering this resulted in 1,473,121 unique CpG sites. Sites with 100% methylation rates ranged from 9% to 11%.

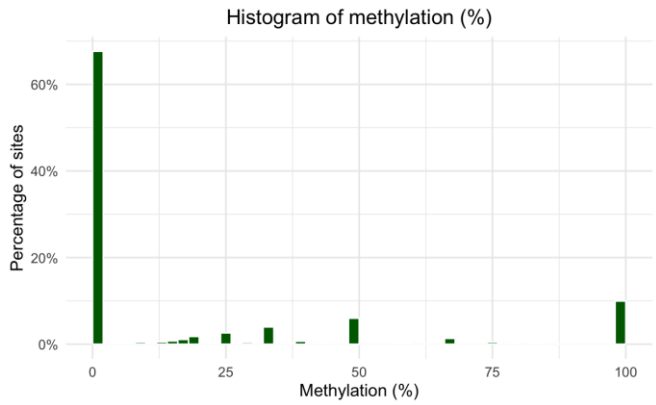

Figure 10. Percentage of methylation per base of sample 'S.3'.

While genetic data revealed pronounced island-specific structuring, a PCA on epigenetic variation did not show such clustering, suggesting weaker or more heterogeneous epigenetic differentiation among islands (Figure 11). In corroboration with previous genetic findings, no clustering according to morphotype could be detected across both islands or within islands (Figure 11).

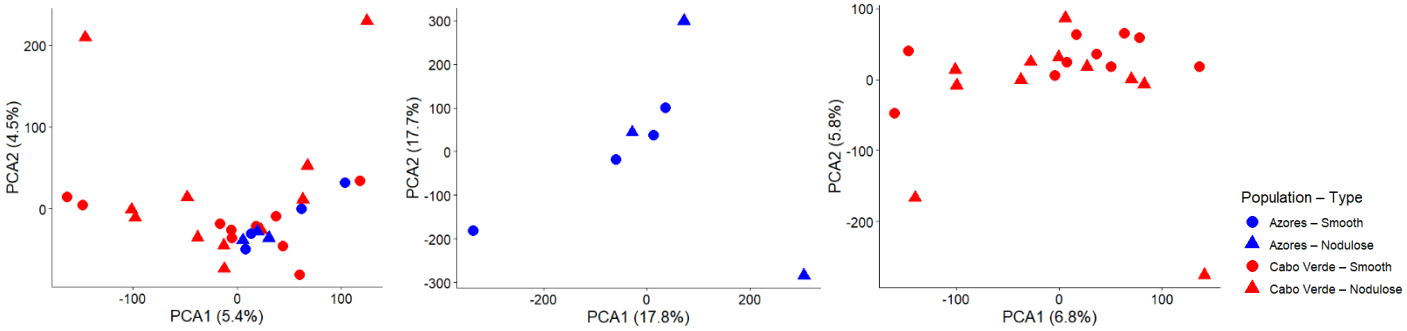

Figure 11. PCA of epigenetic variation of nodulose (triangle) and smooth (circle) specimens of the Azores (blue) and Cabo Verde (red). The percentage of variation explained by each axis is given between brackets. Left panel includes all specimens, middle panel only specimens of Azores and right panel only those of Cabo Verde.

Next, we calculated the per-sample mean methylation weighted by coverage ("global methylation"). To assess differences in global methylation levels between both morphotypes we ran a general linear model with global methylation as dependent variable and island and morphotype as independent variables. Global methylation levels did not differ between morphotypes ($F_{1,23}$=1.17, p=0.29) (Figure 12).

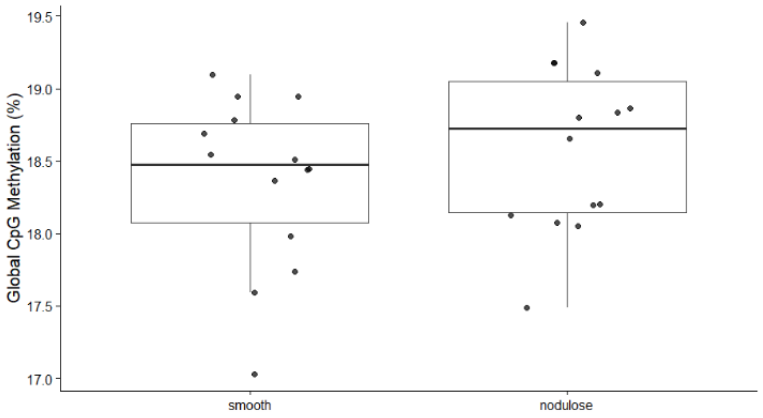

Figure 12. Boxplot of global methylation level in the 'smooth' and 'nodulose' morphotype.

As we did not necessarily expect to observe overall differences in methylation, we subsequently explored site-specific differences in methylation between both shell morphotypes using t-tests. A frequency plot of unadjusted p-values resulted in a rather uniform distribution which indicates that the majority of sites were not differentially methylated (Figure 13, left panel). When we zoomed in on sites with at least 10% differential methylation (substantial effects), a volcano plot highlighted however a small number of putative differentially methylated sites (n= 1589) (Figure 13, right panel). Most CpG sites clustered near zero on the x-axis, indicating minimal methylation changes, whereas a subset of sites exhibits larger positive or negative differences, reflecting both hypermethylation and hypomethylation of the nodulose or smooth morphotype. These significant sites are concentrated at the right or left top of the volcano plot, demonstrating strong statistical support for differential methylation. Overall, the plot highlights that while the majority of the genome shows little differential methylation, specific sites show substantial and significant methylation differences between the morphotypes.

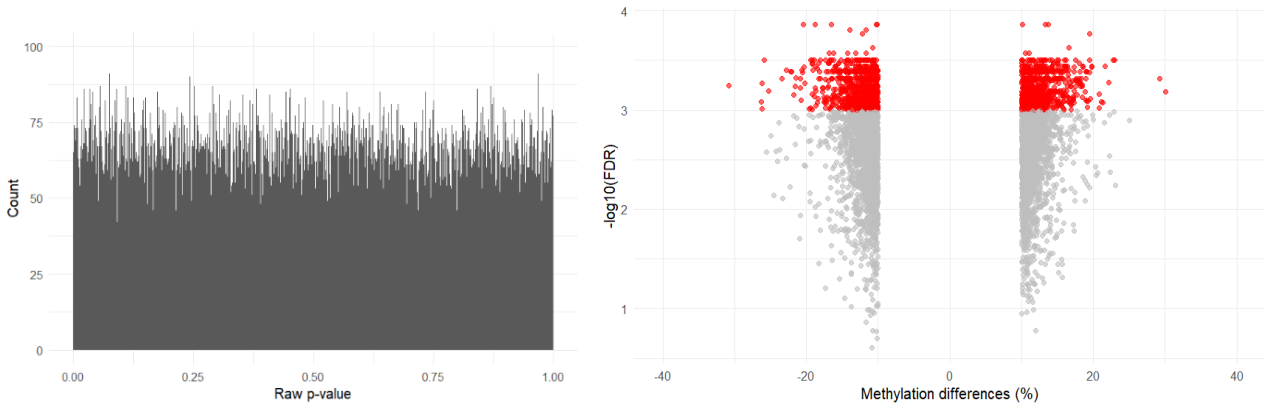

Figure 13. Morphotype-specific differences in methylation levels. Distribution of unadjusted p-values (left panel). Volcano plot depicting methylation differences (%) versus significance level (right panel). Red dots denote significantly differentially methylated (FDR<0.05).

Finally, a DAPC analysis showed that islands could be distinguished based on epigenomic variation, though the effect was weaker than that observed with genomic variation (requiring more PCA axes). Interestingly, while genomic variation failed to separate morphotypes, epigenomic variation succeeded, albeit less distinctly than the separation between islands (Figure 14). As a cautionary note, these analyses were based on 21 PCA axes, which retained 80% of the variation, whereas only fewer PCA axes were plausible in the genomic analysis due to the smaller dataset.

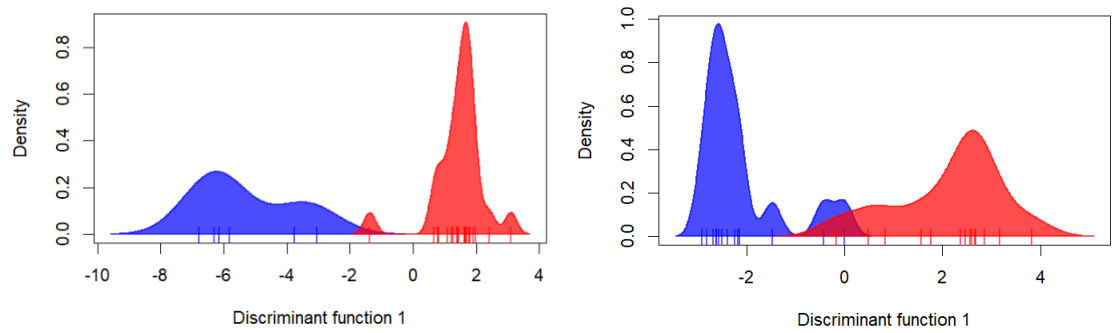

Figure 14. Density plot of the first discriminant axis of the DAPC analysis based on epigenomic variation depicting differentiation among islandss (left figure) and morphotypes (right figure).

4.5 Reduced representation bisulphite sequencing

To verify whether reduced representation bisulphite sequencing (RRBS) resulted in similar epigenomic patterns as those of WGBS (yet at a lower cost as only a fraction of the genome need to be sequenced), we constructed two RRBS libraries of samples that were previously processed (S8 and S10, see Table I). The RRBS libraries resulted in 19203 sites of which 14483 (75%) were shared with the WGBS database. RRBS and WGBS methylation estimates at shared CpG sites were highly concordant (Pearson correlation coefficient of r_p= 0.77 (p<0.001) and r_p= 0.72 (p<0.001) for respectively sample S8 and S10). Mean per-sample methylation for RRBS and WGBS was respectively 21.22% and 21.54% for sample S8 and 20.69% and 19.96% for sample S10. When comparing methylation estimates from both technologies, the smoothed curve closely followed the theoretical line representing perfect correlation. At higher methylation levels, RRBS tended to yield slightly higher estimates than WGBS (Figure 15).

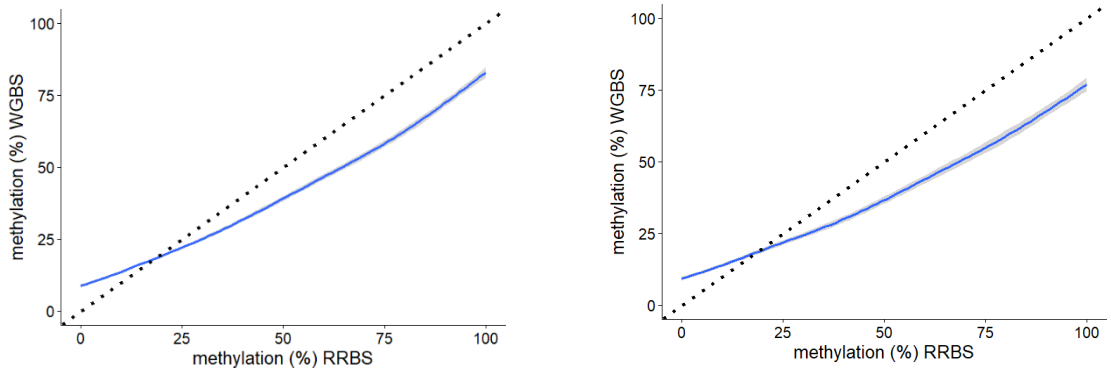

Figure 15. Correlation plot for methylation estimates of identical sites constructed by RRBS and WGBS for samples "S8" (left panel) and 'S10" (right panel). Blue line is the smoothed curve across all sites, black dotted line depicts a theoretical perfect correlation.

In conclusion, epigenomic profiles derived from RRBS libraries were highly concordant with those obtained from WGBS. This indicates that RRBS represents a robust alternative to WGBS in studies where increased sample size (RRBS) is prioritized over comprehensive genome-wide coverage (WGBS).

4.6 Methylation patterns of less optimal preserved museum specimens

We explored methylation patterns in museum samples of *Tectarius striatus* (n=7) stored at suboptimal conditions (i.e. sampled more than three decades ago and stored on ethanol at room temperature). Frequency plots of the percentage of methylated bases in ethanol preserved samples were comparable to those preserved in optimal conditions (Figure 10, Figure 16).

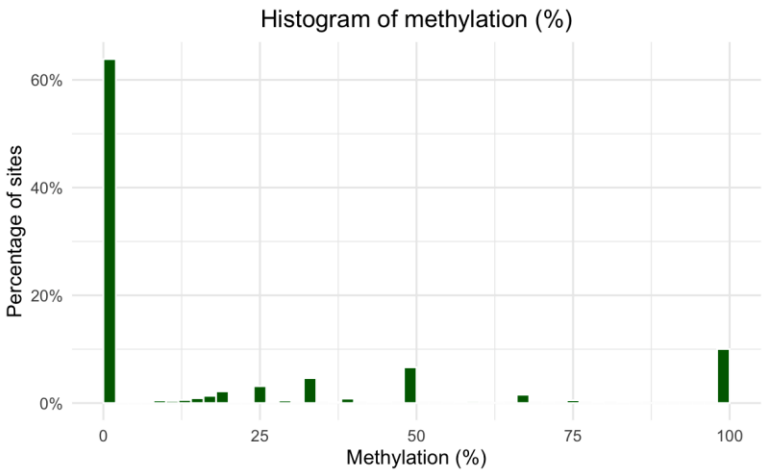

Figure 16. Percentage of methylation per base of sample 'LibSE20250619_1'.

We further compared the percentage of methylation per site with those of samples preserved under optimal conditions (stored at -80°C, flash-frozen using liquid nitrogen upon sampling, see 4.4.2). After stringent filtering (sites with a coverage below 10X and those that have more than 99.9th percentile of coverage in each sample were discarded), linking both databases resulted in 994666 shared CpG sites. To explore to what extent inferior storage conditions could lead to an up- or downwards bias in methylation calling, we extracted the maximum and minimum methylation rates per site from the methylation database of optimal preserved samples. These upper and lower limits were set as the expected methylation range per site. Methylation rates in ethanol preserved samples above or below this range were defined as respectively hyper- and hypomethylated sites. Overall, only 2.89% and 3.04% of all sites were highlighted as respectively hyper- and hypomethylated, while 94.1% of the sites showed methylation values well within the expected range. Moreover, these hyper- and hypomethylated sites were randomly distributed across sites and individuals (Figure 17, Table VII).

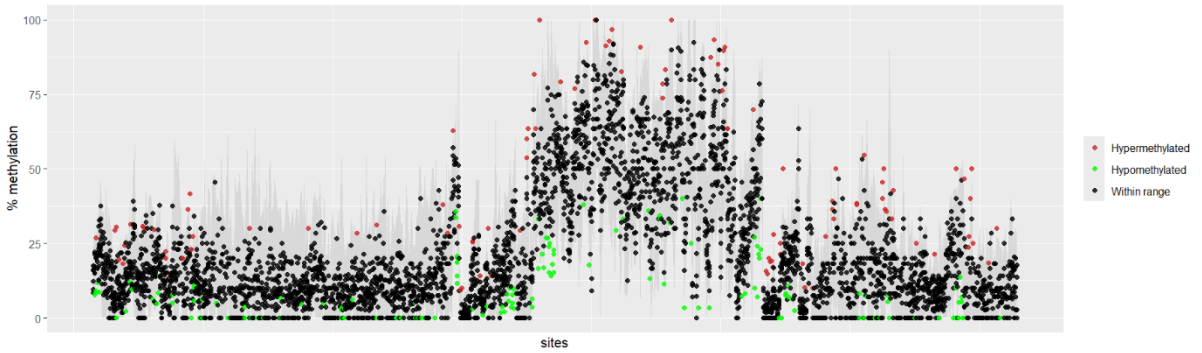

Figure 17. Percentage of methylation per site in ethanol preserved museum samples. Grey bar represent the expected methylation range (based on optimal preserved samples). Dots represent methylation rates for each ethanol preserved sample: red and green colours denote respectively hypermethylated (above expected range)

and hypomethylated (below expected range) sites, black colour denotes methylation rates within the expected range. For illustrative purposes only 700 sites are plotted.

TABLE VII. Hypo- and hypermethylation rates (percentage of all sites) of seven ethanol preserved samples.

sample	hyper	hypo	within range
LibSE20250619_1	2.99	2.34	94.70
LibSE20250619_2	1.63	5.97	92.40
LibSE20250619_3	3.45	1.97	94.60
LibSE20250619_4	3.53	2.00	94.50
LibSE20250619_5	1.97	3.91	94.10
LibSE20250619_7	3.39	2.43	94.20
LibSE20250619_8	3.24	2.65	94.10

In conclusion, we found no evidence that less optimal preserved museum samples showed clear signatures of hypo- or hypermethylation as methylation rates of these samples seemed to remain comparable to those preserved under the highest preservation standards. Hence, it seems that methylation patterns remain unaffected by inferior preservation conditions and these type of collections therefore remain a valuable source in future museum epigenomic studies.

Conclusions and recommendations

- Epigenomic wet-lab protocols and bioinformatic pipelines were successfully established for the analysis of museum specimens. The expertise acquired through this work can now be readily disseminated to other researchers at RBINS via JEMU, which serves as the Institute's molecular information hub. This has already led to the initiation of a new collaboration and a joint grant application.

- We further demonstrated that specimens preserved under suboptimal conditions can nonetheless yield high-quality epigenomic data, confirming their value as a resource for museum-based epigenomic research. These results justify and encourage further investment in the exploration of a wider diversity of museum collection types.

- While the *Calosoma* genome appears to lack DNA methylation, the investigation of open chromatin structures represents a promising alternative avenue for epigenomic analysis.

- Adaptive shell morphology in snails showed no detectable genetic basis, but instead appears to be primarily driven by epigenetic mechanisms. Currently efforts are focused on assembling an improved reference genome using long-read sequencing approaches, drawing on protocols shared by experts in snail genomics. This will increase genome-wide coverage and resolution and enable the investigation of structural variation as a potential molecular driver of shell morphology. Interpretation of the epigenomic data will be further strengthened through the integration of RNAseq data, which is currently ongoing.

5. DISSEMINATION AND VALORISATION

- Janne Swaegers presented the MUTER project on "TaxPhylDay" at RBINS, 18th of April 2024.
- Introduction of MUTER project: methodology, technology and research possibilities. Evolunch meeting to promote collaborations with JEMU and implementation of an epigenomic component in future research of researchers at RBINS, 16th of November 2023.
- The role of plasticity during adaptation: thermal responses in a southward expanding damselfly and epigenomic explorations in a polymorphic periwinkle. Seminar at Environmental and Evolutionary Biology Research Unit, University of Namur, 6th of February 2026

6. PUBLICATIONS

Chromosomal inversions from an initial ecotypic divergence drive a gradual repeated radiation of Galápagos beetles, 2024, **Vangestel C.**, **Swaegers J.**, De Corte Z., Dekoninck W., Gharbi K., Gillespie R., Vandekerckhove M., Van Belleghem S.M., **Hendrickx F.**, *Science Advances*, 10, eadk7906.

7. ACKNOWLEDGEMENTS

We are especially indebted to Prof Dr. Katerina Guschanski (University of Uppsala, University of Edinburgh) for her constructive advice and valuable insights on our study.
We are grateful to the follow-up committee for their valuable advice and constructive feedback during the course of the project:
- Dr. Tine Huyse (RMCA)
- Prof. Dr. Sofie Derycke (ILVO)
- Prof. Dr. Steven Janssen (Botanical Garden of Meisse)

8. REFERENCES

Artemov, A. V., Mugue, N. S., Rastorguev, S. M., Zhenilo, S., Mazur, A. M., Tsygankova, S. V., Boulygina, E. S., Kaplun, D., Nedoluzhko, A. V., Medvedeva, Y. A., & Prokhortchouk, E. B. (2017). Genome-Wide DNA Methylation Profiling Reveals Epigenetic Adaptation of Stickleback to Marine and Freshwater Conditions. *Molecular Biology and Evolution*, *34*(9), 2203–2213. https://doi.org/10.1093/molbev/msx156

Bi, K., Linderoth, T., Vanderpool, D., Good, J. M., Nielsen, R., & Moritz, C. (2013). Unlocking the vault: Next-generation museum population genomics. *Molecular Ecology*, *22*(24), 6018–6032. https://doi.org/10.1111/mec.12516

Bossdorf, O., Richards, C. L., & Pigliucci, M. (2008). Epigenetics for ecologists. *Ecology Letters*, *11*(2), 106–115. https://doi.org/10.1111/j.1461-0248.2007.01130.x

Buenrostro, J. D., Wu, B., Chang, H. Y., & Greenleaf, W. J. (2015). ATAC-seq: A Method for Assaying Chromatin Accessibility Genome-Wide. *Current Protocols in Molecular Biology*, *109*(1). https://doi.org/10.1002/0471142727.mb2129s109

Carøe, C., Gopalakrishnan, S., Vinner, L., Mak, S. S. T., Sinding, M. H. S., Samaniego, J. A., Wales, N., Sicheritz-Pontén, T., & Gilbert, M. T. P. (2018). Single-tube library preparation for degraded DNA. *Methods in Ecology and Evolution*, *9*(2), 410–419. https://doi.org/10.1111/2041-210X.12871

Cavalli, G., & Heard, E. (2019). Advances in epigenetics link genetics to the environment and disease. *Nature*, *571*(7766), 489–499. https://doi.org/10.1038/s41586-019-1411-0

Clark, M. S., Peck, L. S., Arivalagan, J., Backeljau, T., Berland, S., Cardoso, J. C. R., Caurcel, C., Chapelle, G., De Noia, M., Dupont, S., Gharbi, K., Hoffman, J. I., Last, K. S., Marie, A., Melzner, F., Michalek, K., Morris, J., Power, D. M., Ramesh, K., … Harper, E. M. (2020). Deciphering mollusc shell production: The roles of genetic mechanisms through to ecology, aquaculture and biomimetics. *Biological Reviews*, *95*(6), 1812–1837. https://doi.org/10.1111/brv.12640

Clark, M. S., Thorne, M. A. S., King, M., Hipperson, H., Hoffman, J. I., & Peck, L. S. (2018). Life in the intertidal: Cellular responses, methylation and epigenetics. *Functional Ecology*, *32*(8), 1982–1994. https://doi.org/10.1111/1365-2435.13077

De Busschere, C., Baert, L., Van Belleghem, S. M., Dekoninck, W., & Hendrickx, F. (2012). Parallel phenotypic evolution in a wolf spider radiation on Galápagos: Parallel evolution on Galápagos. *Biological Journal of the Linnean Society*, *106*(1), 123–136. https://doi.org/10.1111/j.1095-8312.2011.01848.x

De Busschere, C., Van Belleghem, S. M., & Hendrickx, F. (2015). Inter and intra island introgression in a wolf spider radiation from the Galápagos, and its implications for parallel evolution. *Molecular Phylogenetics and Evolution*, *84*, 73–84. https://doi.org/10.1016/j.ympev.2014.11.004

De Wolf, H., Backeljau, T., Medeiros, R., & Verhagen, R. (1997). Microgeographical shell variation in Littorina striata , a planktonic developing periwinkle. *Marine Biology*, *129*(2), 331–342. https://doi.org/10.1007/s002270050173

De Wolf, H., Backeljau, T., Van Dongen, S., & Verhagen, R. (1998). Large-scale patterns of shell variation in Littorina striata, a planktonic developing periwinkle from Macaronesia (Mollusca: Prosobranchia). *Marine Biology*, *131*(2), 309–317. https://doi.org/10.1007/s002270050324

De Wolf, H., Backeljau, T., & Verhagen, R. (1998). Spatio-temporal genetic structure and gene flow between two distinct shell morphs of the planktonic developing periwinkle Littorina striata (Mollusca: Prosobranchia). *Marine Ecology Progress Series*, *163*, 155–163.

Desender, K., & de Dijn, B. (1990). The Calosoma species (Coleoptera, Carabidae) of the Galápagos archipelago. II. Discriminant analyses and species identification key. *Bulletin of the Royal Belgian Institute of Natural Sciences - Entomology*, *60*, 55–68.

Fallet, M., Luquet, E., David, P., & Cosseau, C. (2020). Epigenetic inheritance and intergenerational effects in mollusks. *Gene*, *729*, 144166. https://doi.org/10.1016/j.gene.2019.144166

Feil, R., & Fraga, M. F. (2012). Epigenetics and the environment: Emerging patterns and implications. *Nature Reviews Genetics*, *13*(2), 97–109. https://doi.org/10.1038/nrg3142

Flores, K. B., Wolschin, F., & Amdam, G. V. (2013). The Role of Methylation of DNA in Environmental Adaptation. *Integrative and Comparative Biology*, *53*(2), 359–372. https://doi.org/10.1093/icb/ict019

Gibbin, E. M., Massamba N'Siala, G., Chakravarti, L. J., Jarrold, M. D., & Calosi, P. (2017). The evolution of phenotypic plasticity under global change. *Scientific Reports*, *7*(1), 17253. https://doi.org/10.1038/s41598-017-17554-0

Grehl, C., Kuhlmann, M., Becker, C., Glaser, B., & Grosse, I. (2018). How to Design a Whole-Genome Bisulfite Sequencing Experiment. *Epigenomes*, *2*(4), 21. https://doi.org/10.3390/epigenomes2040021

Hahn, E. E., Grealy, A., Alexander, M., & Holleley, C. E. (2020). Museum Epigenomics: Charting the Future by Unlocking the Past. *Trends in Ecology & Evolution*, *35*(4), 295–300. https://doi.org/10.1016/j.tree.2019.12.005

Hendrickx, F., Backeljau, T., Dekoninck, W., Van Belleghem, S. M., Vandomme, V., & Vangestel, C. (2015). Persistent inter- and intraspecific gene exchange within a parallel radiation of caterpillar hunter beetles (*C alosoma* sp.) from the G alápagos. *Molecular Ecology*, *24*(12), 3107–3121. https://doi.org/10.1111/mec.13233

Holmes, M. W., Hammond, T. T., Wogan, G. O. U., Walsh, R. E., LaBarbera, K., Wommack, E. A., Martins, F. M., Crawford, J. C., Mack, K. L., Bloch, L. M., & Nachman, M. W. (2016). Natural history collections as windows on evolutionary processes. *Molecular Ecology*, *25*(4), 864–881. https://doi.org/10.1111/mec.13529

Jablonka, E. (2017). The evolutionary implications of epigenetic inheritance. *Interface Focus*, *7*(5), 20160135. https://doi.org/10.1098/rsfs.2016.0135

Jimenez-Useche, I., & Yuan, C. (2012). The Effect of DNA CpG Methylation on the Dynamic Conformation of a Nucleosome. *Biophysical Journal*, *103*(12), 2502–2512. https://doi.org/10.1016/j.bpj.2012.11.012

Johannesson, B., & Johannesson, K. (1996). Population differences in behaviour and morphology in the snail Littorina saxatilis: Phenotypic plasticity or genetic differentiation? *Journal of Zoology*, *240*, 475–493.

Jordaens, K., Van Riel, P., Frias Martins, A. M., & Backeljau, T. (2009). Speciation on the Azores islands: Congruent patterns in shell morphology, genital anatomy, and molecular markers in endemic land snails (Gastropoda, Leptaxinae): SPECIATION IN AZOREAN LAND SNAILS. *Biological Journal of the Linnean Society*, *97*(1), 166–176. https://doi.org/10.1111/j.1095-8312.2008.01197.x

Kess, T., & Boulding, E. G. (2019). Genome-wide association analyses reveal polygenic genomic architecture underlying divergent shell morphology in Spanish *Littorina saxatilis* ecotypes. *Ecology and Evolution*, *9*(17), 9427–9441. https://doi.org/10.1002/ece3.5378

Kharouba, H. M., Lewthwaite, J. M. M., Guralnick, R., Kerr, J. T., & Vellend, M. (2019). Using insect natural history collections to study global change impacts: Challenges and opportunities. *Philosophical Transactions of the Royal Society B: Biological Sciences*, *374*(1763), 20170405. https://doi.org/10.1098/rstb.2017.0405

Krueger, F., & Andrews, S. R. (2011). Bismark: A flexible aligner and methylation caller for Bisulfite-Seq applications. *Bioinformatics*, *27*(11), 1571–1572. https://doi.org/10.1093/bioinformatics/btr167

Le Pennec, G., Butlin, R. K., Jonsson, P. R., Larsson, A. I., Lindborg, J., Bergström, E., Westram, A. M., & Johannesson, K. (2017). Adaptation to dislodgement risk on wave-swept rocky shores in the snail Littorina saxatilis. *PLOS ONE*, *12*(10), e0186901. https://doi.org/10.1371/journal.pone.0186901

Llamas, B., Holland, M. L., Chen, K., Cropley, J. E., Cooper, A., & Suter, C. M. (2012). High-Resolution Analysis of Cytosine Methylation in Ancient DNA. *PLoS ONE*, *7*(1), e30226. https://doi.org/10.1371/journal.pone.0030226

MacLean, H. J., Nielsen, M. E., Kingsolver, J. G., & Buckley, L. B. (2018). Using museum specimens to track morphological shifts through climate change. *Philosophical Transactions of the Royal Society B: Biological Sciences*, *374*, 20170404.

McMahon, R., & Whitehead, B. (1987). Environmental induction of shell morphometric variation in the European stream limpet, Ancylus fluviatilis (Muller) (Pulmonata: Basommatophora). *American Malacological Bulletin*, *5*, 105–124.

Metzker, M. L. (2010). Sequencing technologies—The next generation. *Nature Reviews Genetics*, *11*(1), 31–46. https://doi.org/10.1038/nrg2626

Muyle, A., Ross-Ibarra, J., Seymour, D. K., & Gaut, B. S. (2021). Gene body methylation is under selection in *Arabidopsis thaliana*. *Genetics*, *218*(2), iyab061. https://doi.org/10.1093/genetics/iyab061

Riel, P. V., Jordaens, K., Houtte, N. V., Martins, A. M. F., Verhagen, R., & Backeljau, T. (2005). Molecular systematics of the endemic Leptaxini (Gastropoda: Pulmonata) on the Azores islands. *Molecular Phylogenetics and Evolution*, *37*(1), 132–143. https://doi.org/10.1016/j.ympev.2005.03.019

Rubi, T. L., Knowles, L. L., & Dantzer, B. (2020). Museum epigenomics: Characterizing cytosine methylation in historic museum specimens. *Molecular Ecology Resources*, *20*(5), 1161–1170. https://doi.org/10.1111/1755-0998.13115

Schübeler, D. (2015). Function and information content of DNA methylation. *Nature*, *517*(7534), 321–326. https://doi.org/10.1038/nature14192

Skinner, M. K., Gurerrero-Bosagna, C., Haque, M. M., Nilsson, E. E., Koop, J. A. H., Knutie, S. A., & Clayton, D. H. (2014). Epigenetics and the Evolution of Darwin's Finches. *Genome Biology and Evolution*, *6*(8), 1972–1989. https://doi.org/10.1093/gbe/evu158

Sproul, J. S., & Maddison, D. R. (2017). Sequencing historical specimens: Successful preparation of small specimens with low amounts of degraded DNA. *Molecular Ecology Resources*, *17*(6), 1183–1201. https://doi.org/10.1111/1755-0998.12660

Thorson, J. L. M., Smithson, M., Beck, D., Sadler-Riggleman, I., Nilsson, E., Dybdahl, M., & Skinner, M. K. (2017). Epigenetics and adaptive phenotypic variation between habitats in an asexual snail. *Scientific Reports*, *7*(1), 14139. https://doi.org/10.1038/s41598-017-14673-6

Van Belleghem, S. M., Vangestel, C., De Wolf, K., De Corte, Z., Möst, M., Rastas, P., De Meester, L., & Hendrickx, F. (2018). Evolution at two time frames: Polymorphisms from an ancient singular divergence event fuel contemporary parallel evolution. *PLOS Genetics*, *14*(11), e1007796. https://doi.org/10.1371/journal.pgen.1007796

Van Den Broeck, H., Breugelmans, K., De Wolf, H., & Backeljau, T. (2008). Completely disjunct mitochondrial DNA haplotype distribution without a phylogeographic break in a planktonic developing gastropod. *Marine Biology*, *153*(3), 421–429. https://doi.org/10.1007/s00227-007-0820-z

Vangestel, C., Swaegers, J., De Corte, Z., Dekoninck, W., Gharbi, K., Gillespie, R., Vandekerckhove, M., Van Belleghem, S. M., & Hendrickx, F. (2024). Chromosomal inversions from an initial ecotypic divergence drive a gradual repeated radiation of Galápagos beetles. *Science Advances*, *10*(22), eadk7906. https://doi.org/10.1126/sciadv.adk7906

Vernaz, G., Malinsky, M., Svardal, H., Du, M., Tyers, A. M., Santos, M. E., Durbin, R., Genner, M. J., Turner, G. F., & Miska, E. A. (2021). Mapping epigenetic divergence in the massive radiation of Lake Malawi cichlid fishes. *Nature Communications*, *12*(1), 5870. https://doi.org/10.1038/s41467-021-26166-2

Xu, G., Lyu, J., Li, Q., Liu, H., Wang, D., Zhang, M., Springer, N. M., Ross-Ibarra, J., & Yang, J. (2020). Evolutionary and functional genomics of DNA methylation in maize domestication and improvement. *Nature Communications*, *11*(1), 5539. https://doi.org/10.1038/s41467-020-19333-4

Yeates, D. K., Zwick, A., & Mikheyev, A. S. (2016). Museums are biobanks: Unlocking the genetic potential of the three billion specimens in the world's biological collections. *Current Opinion in Insect Science*, *18*, 83–88. https://doi.org/10.1016/j.cois.2016.09.009